

Influence of Copper(I) Halides on the Reactivity of Aliphatic Carbodiimides [†]

Valentina Ferraro * and Marco Bortoluzzi

Dipartimento di Scienze Molecolari e Nanosistemi, Università Ca' Foscari, Via Torino 155, 30170 Mestre (VE), Italy; markos@unive.it

* Correspondence: valentina.ferraro@unive.it; Tel.: +39-041-234-8651

[†] Presented at the 24th International Electronic Conference on Synthetic Organic Chemistry, 15 November–15 December 2020; Available online: <https://ecsoc-24.sciforum.net/>.

Abstract: The influence of copper(I) halides CuX (X = Cl, Br, I) on the electronic structure of *N,N'*-diisopropylcarbodiimide (DICDI) and *N,N'*-dicyclohexylcarbodiimide (DCC) was investigated by means of computational DFT (density functional theory) methods. The coordination of the considered carbodiimides occurs by one of the nitrogen atoms, with the formation of linear complexes having a general formula of [CuX(carbodiimide)]. Besides varying the carbon–nitrogen bond lengths, the thermodynamically favourable interaction with Cu(I) reduces the electron density on the carbodiimides and alters the energies of the {NCN}-centred, unoccupied orbitals. A small dependence of these effects on the choice of the halide was observable. The computed Fukui functions suggested negligible interaction of Cu(I) with incoming nucleophiles, and the reactivity of carbodiimides was altered by coordination mainly because of the increased electrophilicity of the {NCN} fragments.

Keywords: carbodiimides; copper(I) halides; DFT calculations; population analyses

Citation: Ferraro, V.; Bortoluzzi, M. Influence of Copper(I) Halides on the Reactivity of Aliphatic Carbodiimides. *Chem. Proc.* **2021**, *3*, 20. <https://doi.org/10.3390/ecsoc-24-08096>

Academic Editors: Julio A. Seijas and M. Pilar Vázquez-Tato

Published: 13 November 2020

Publisher's Note: MDPI stays neutral with regard to jurisdictional claims in published maps and institutional affiliations.



Copyright: © 2020 by the authors. Licensee MDPI, Basel, Switzerland. This article is an open access article distributed under the terms and conditions of the Creative Commons Attribution (CC BY) license (<http://creativecommons.org/licenses/by/4.0/>).

1. Introduction

Carbodiimides are heteroallenes that play a crucial role in synthetic organic chemistry and biochemistry. Selected examples of the most important reactions are oligomerizations and polymerizations, cycloadditions, insertions, and interactions with nucleophiles. As an example, carbodiimides are used with dimethyl sulfoxide for the mild oxidation of alcohols to ketones. Carbodiimides find application in several condensation reactions, and the most noticeable example is the formation of peptide bonds from carboxylic acids and amines. As dehydrating agents, carbodiimides are used in reactions such as the conversion of primary amides to nitriles and of β -hydroxy ketones to α,β -unsaturated ketones, and they are involved in the synthesis of β -lactam antibiotics and nucleotides [1–4].

The most widely exploited carbodiimides in organic synthesis are diisopropyl carbodiimide (DICDI) and dicyclohexylcarbodiimide (DCC). The electrophilicity of carbodiimides can be enhanced by the addition of copper(I) halides to the reaction medium. For instance, the reaction of β -hydroxy ketones with DCC/CuCl affords α,β -unsaturated ketones, whereas α -cyclopropyl ketones can be obtained using γ -hydroxy ketones as reactants [5,6]. DCC/CuCl reacts with 2-hydroxyimines and nitroaldols to afford 2,3-enamines and nitroalkenes [7,8]. Isoureas, useful alkylating agents also involved in the preparation of heterocyclic compounds, are commonly obtained from the reaction of carbodiimides with alcohols in the presence of catalytic CuX [9–15]. The mild reaction conditions typical of Cu(I) catalysis provide an alternative and selective synthetic approach with respect to the utilization of Brønsted acids that can promote oligomerization or interfere with other functional groups. For example, aliphatic carbodiimides undergo rapid

dimerization catalyzed by tetrafluoroboric acid at room temperature to give salts of the cyclodimer 1,3-dialkyl-2,4-bisalkylimino-1,3-diazetidines [16].

The catalytic action of copper halides apparently consists in the formation of coordination complexes with carbodiimides, but scarce experimental evidence is provided in the literature. In this work, the interaction of DICDI and DCC with CuX (X = Cl, Br, I) was investigated by means of DFT calculations, and the influence of coordination on the electronic structure of carbodiimides was studied by several population analyses.

2. Methods

The computational geometry optimizations of DICDI, DCC, and the corresponding CuX complexes were carried out without symmetry constraints, using the range-separated hybrid functional ω B97X [17–19] and the def2 split-valence polarized basis set of Ahlrichs and Weigend, with relativistic ECP (effective core potential) for iodine (28 electrons included in the pseudopotential) [20,21]. The restricted approach was applied for the free carbodiimides and the neutral copper complexes, whereas unrestricted single point calculations were carried out for the corresponding mono-anionic species. The electron densities were used for the plot of $f_{\nu}(r)$ Fukui functions [22]. The C-PCM conductor-like polarizable continuum model was added to the ω B97X calculations, considering dichloromethane as a continuous medium (dielectric constant = 8.93, refractive index = 1.424) [23,24]. The software used was ORCA 4.2.0 [25,26].

The output, converted to molden format, was used for Mulliken and Hirshfeld charge distributions [27,28], Mayer and Wiberg bond order analysis [29,30], AIM analysis [31], electrostatic potential calculations, charge decomposition analysis (CDA), and extended charge decomposition analysis (ECDA) [32,33]. The software used was Multiwfn, version 3.5 [34]. All the calculations were performed with Intel Xeon-based x84-64 workstations.

3. Results and Discussion

The optimized geometries of DICDI, DCC, and the Cu(I) complexes [CuX(DICDI)] and [CuX(DCC)] are superimposed in Figure 1. All the attempts were afforded as stationary point linear complexes with the carbodiimide κ^1 -coordinated to Cu(I) by a nitrogen atom, ruling out the possibility of η^2 -coordination by the C=N bonds.

Selected bond lengths are compared in Table 1. As was observed, the coordination affected the carbon–nitrogen bond lengths, with the C=N and C–N bonds involving the coordinating nitrogen atom that become slightly longer, whereas the other C=N bond was shorter in the coordination compounds with respect to the free carbodiimides. These variations, comparable between DICDI and DCC, do not depend upon the nature of X. The N=C=N angle was not influenced by coordination, and it falls in the 174–175° range for all the considered species. The N–Cu distances (in the 1.929–1.938 Å range) were similar among all the complexes, and the slightly longer values corresponded to the heavier halide complexes. Accordingly, the Gibbs energy variations for the carbodiimide + CuX → [CuX(carbodiimide)] reactions were more negative for X = Cl (average $\Delta G = -39.5$ kcal mol⁻¹) with respect to X = Br (average $\Delta G = -38.5$ kcal mol⁻¹) and X = I (average $\Delta G = -36.8$ kcal mol⁻¹). Such a trend can be explained on the basis of the softness of Cu(I) as a metal centre and of the increasing softness of the halides along their group.

The variations in the carbon–nitrogen bonds were well highlighted by the Mayer and Wiberg bond orders, reported in Table 2. The C1–N3 interaction lost part of its double bond nature, and the weakening of the N3–C5 bond was confirmed. According to the computed bond lengths, the C1–N2 bond was enforced by the coordination of the carbodiimides to CuX. Further confirmation comes from the electron density (ρ) and potential energy density (V) values at carbon–nitrogen (3,-1) bond critical points (b.c.p.), reported in Table 3. The ρ values for the C1–N3 and N3–C5 b.c.p. decrease (and the

corresponding V values become less negative) moving from free to coordinated carbodiimides, whereas the opposite behaviour is shown by the C1–N2 b.c.p.

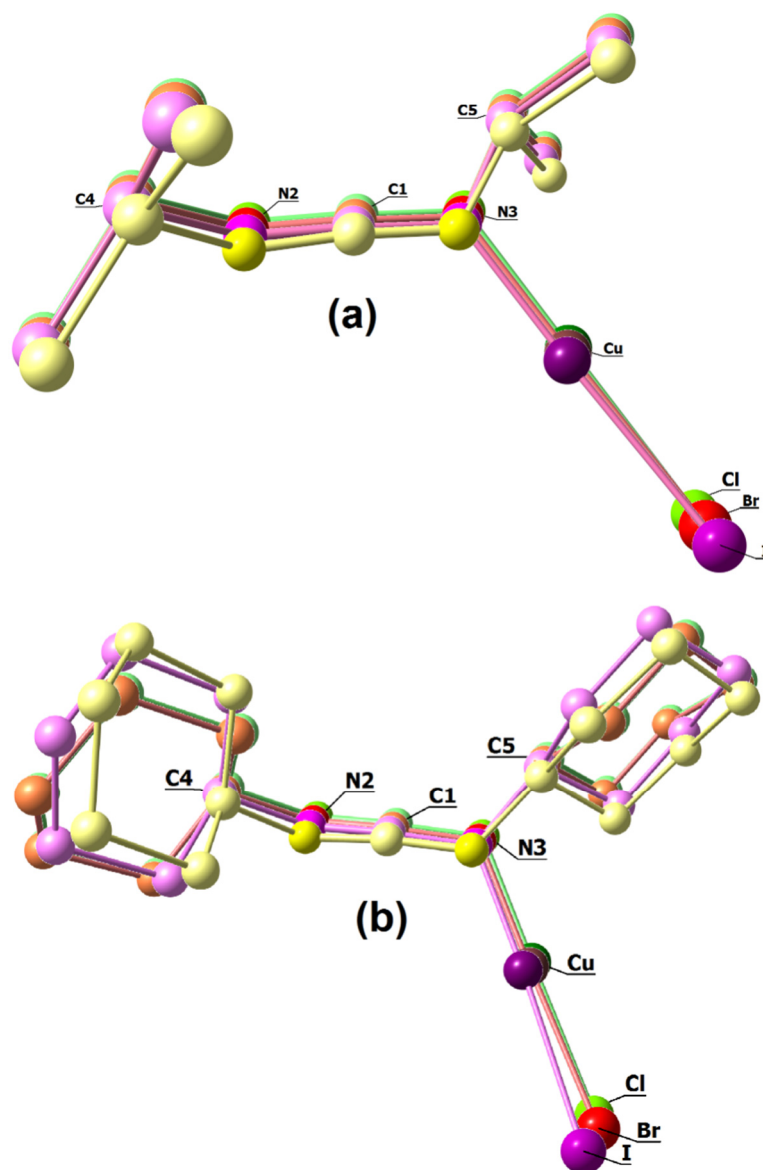


Figure 1. DFT-optimized structures of: (a) diisopropylcarbodiimide (DICDI) and $[\text{CuX}(\text{DICDI})]$; (b) dicyclohexylcarbodiimide (DCC) and $[\text{CuX}(\text{DCC})]$. Free carbodiimides, yellow tones; CuCl complexes, green tones; CuBr complexes, red tones; CuI complexes, violet tones. Hydrogen atoms were omitted for clarity. Selected captions were added for clarity.

Table 1. Selected computed bond lengths (\AA) for carbodiimides and CuX complexes.

Bond	DICDI	$[\text{CuCl}(\text{DICDI})]$	$[\text{CuBr}(\text{DICDI})]$	$[\text{CuI}(\text{DICDI})]$
C1–N2	1.217	1.193	1.193	1.193
C1–N3	1.215	1.243	1.243	1.243
N2–C4	1.478	1.470	1.470	1.470
N3–C5	1.471	1.494	1.494	1.494
Bond	DCC	$[\text{CuCl}(\text{DCC})]$	$[\text{CuBr}(\text{DCC})]$	$[\text{CuI}(\text{DCC})]$
C1–N2	1.216	1.192	1.192	1.191
C1–N3	1.217	1.243	1.244	1.244
N2–C4	1.469	1.465	1.464	1.464
N3–C5	1.470	1.489	1.489	1.488

Table 2. Selected computed Mayer bond orders (Wiberg bond orders in parentheses).

Bond	DICDI	[CuCl(DICDI)]	[CuBr(DICDI)]	[CuI(DICDI)]
C1–N2	2.107 (2.393)	2.217 (2.490)	2.217 (2.490)	2.216 (2.491)
C1–N3	2.112 (2.377)	1.692 (2.085)	1.693 (2.086)	1.683 (2.088)
N2–C4	0.864 (1.196)	0.842 (1.164)	0.842 (1.164)	0.842 (1.165)
N3–C5	0.804 (1.179)	0.711 (1.096)	0.710 (1.097)	0.714 (1.098)
Bond	DCC	[CuCl(DCC)]	[CuBr(DCC)]	[CuI(DCC)]
C1–N2	2.072 (2.386)	2.196 (2.487)	2.198 (2.489)	2.199 (2.493)
C1–N3	2.083 (2.379)	1.700 (2.078)	1.700 (2.078)	1.682 (2.077)
N2–C4	0.859 (1.200)	0.867 (1.171)	0.868 (1.171)	0.842 (1.172)
N3–C5	0.837 (1.181)	0.629 (1.102)	0.627 (1.102)	0.664 (1.104)

Table 3. Electron density (ρ) values at carbon–nitrogen (3,-1) bond critical points (b.c.p.). Potential energy density (V) values in parentheses. Data in a.u.

Bond	DICDI	[CuCl(DICDI)]	[CuBr(DICDI)]	[CuI(DICDI)]
C1–N2	0.436 (-1.340)	0.450 (-1.506)	0.450 (-1.505)	0.450 (-1.505)
C1–N3	0.435 (-1.325)	0.418 (-1.159)	0.419 (-1.161)	0.419 (-1.161)
N2–C4	0.248 (-0.410)	0.241 (-0.443)	0.241 (-0.442)	0.241 (-0.443)
N3–C5	0.248 (-0.404)	0.236 (-0.374)	0.236 (-0.374)	0.236 (-0.375)
Bond	DCC	[CuCl(DCC)]	[CuBr(DCC)]	[CuI(DCC)]
C1–N2	0.435 (-1.330)	0.449 (-1.507)	0.450 (-1.509)	0.451 (-1.513)
C1–N3	0.435 (-1.327)	0.418 (-1.153)	0.418 (-1.152)	0.419 (-1.142)
N2–C4	0.249 (-0.414)	0.243 (-0.459)	0.243 (-0.461)	0.243 (-0.463)
N3–C5	0.248 (-0.412)	0.239 (-0.385)	0.239 (-0.385)	0.239 (-0.385)

Primary assessment of the influence of CuX coordination on DICDI and DCC was given by charge decomposition analyses (CDA and ECDA). Net donation of electron density from carbodiimide to CuX, in the 0.237–0.255 a.u. range, was obtained from CDA calculations. This result was confirmed by the ECDA analysis, with computed carbodiimide→CuX donations between 0.374 and 0.415 a.u. Despite the slight reduction in thermodynamic stability of the complexes, an increased electron density transfer was achieved by considering the heavier halides (see Table 4).

The role of coordination was clearly detectable by investigating the molecular orbitals of free and coordinated carbodiimides. In particular, the frontier unoccupied molecular orbitals of DICDI and DCC were mainly localized on the {NCN} fragments, and the bond with CuX introduced σ^* -type interactions with d-type orbitals of Cu(I). The orbital energies were meaningfully lowered, and the LUMO+1 orbitals in free carbodiimides corresponded to the lowest unoccupied molecular orbitals (LUMOs) in [CuX(carbodiimide)]

complexes, with an average energy reduction around 1.5 eV, as depicted in Figure 2 for DICDI and its derivatives. The energy lowering was more accentuated for the heavier halides in accordance with the greater carbodiimide→CuX electron density donation reported in Table 4. The lower energy of {NCN}-centred unoccupied orbitals reasonably makes the overlap with frontier occupied orbitals of electron-rich reactants more efficient. The $\sigma^*(\text{Cu-N})$ nature of LUMO and LUMO+1 in [CuX(carbodiimide)] could favour the Cu–N bond break after the nucleophilic attack, thus helping the catalytic activity of Cu(I) halides.

In spite of the different molecular orbital structures, the comparison of Fukui $f_-(r)$ functions between free and coordinated carbodiimides did not indicate important variations of the molecular regions involved in the interaction with nucleophiles (see, for instance, the inset of Figure 2). In all the cases, the {NCN} fragment was almost exclusively affected, whereas the interaction of Cu(I) with incoming nucleophiles was predicted to be negligible despite the unsaturated coordination sphere of the metal centre. Accordingly, the [CuX(carbodiimide)] molecular orbital diagrams do not show any low energy unoccupied orbitals with proper orientations to interact with electron-rich species. On the basis of these outcomes, it appears that Cu(I) halides essentially act as Lewis acids for the activation of aliphatic carbodiimides.

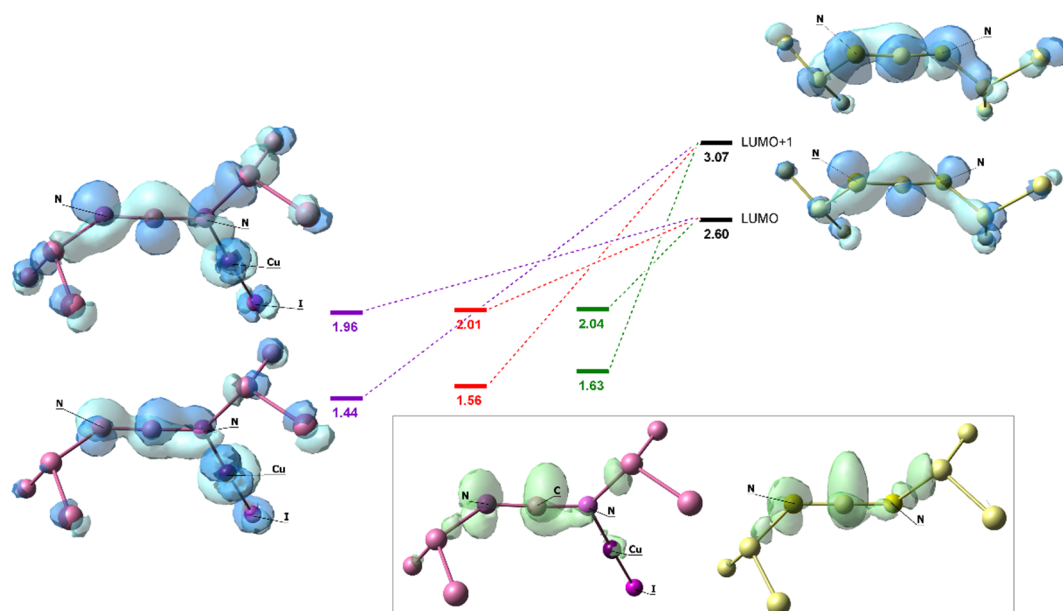


Figure 2. Energy values (eV) of LUMO and LUMO+1 orbitals of DICDI (black levels) and of its CuCl (green levels), CuBr (red levels), and CuI (violet levels) complexes. Plots of the LUMO and LUMO+1 molecular orbitals of DICDI (yellow tones) and of [CuI(DICDI)] (violet tones). Molecular orbital surfaces in blue tones, isovalue = 0.05 a.u. Inset: plots of the Fukui $f_-(r)$ functions for DICDI and [CuI(DICDI)], surfaces in green, isovalue = 0.005 a.u. Hydrogen atoms were omitted for clarity.

Table 4. Charge decomposition analysis (CDA) values for the [CuX(carbodiimide)] complexes. Extended charge decomposition analysis (ECDA) values in parentheses. Data in a.u.

Carbodiimide	CuCl	CuBr	CuI
DICDI	0.237 (0.374)	0.248 (0.391)	0.255 (0.415)
DCC	0.240 (0.379)	0.251 (0.398)	0.254 (0.415)

The influence of coordination can be quantified by studying the partial charge variation in DICDI and DCC after coordination. The Hirshfeld population analyses showed an

increase in the C1 partial charge in the 0.045–0.047 a.u. range. The charge on the coordinating nitrogen atom (N3) was also more positive in the complexes with respect to the free carbodiimides by a comparable quantity (0.040–0.043 a.u.). The most important charge variation affected the non-coordinating nitrogen (N2), with its Hirshfeld charge increasing by 0.074 a.u. in [CuX(DICDI)] complexes and by about 0.082 a.u. in [CuX(DCC)] derivatives. The meaningful increase of electrophilicity of C1 and N2 was confirmed by the Mulliken population analyses, as observable from the data provided in Table 5. The partial charges can be explained from a Lewis structure point of view considering that the donation to Cu(I) causes the partial delocalization of the N2 lone pair on the C1=N2 bond. Such a model is in agreement with the previously described enforcement of the C1=N2 bond caused by coordination. The increased electrophilicity of the {NCN} fragments is well highlighted by the comparison of the electrostatic potentials of free and coordinated carbodiimides, as shown, for example, in Figure 3 for DICDI and its CuCl complex.

Table 5. Selected Hirshfeld partial charges. Mulliken charges in parentheses. Data in a.u.

Atom	DICDI	[CuCl(DICDI)]	[CuBr(DICDI)]	[CuI(DICDI)]
C1	0.152 (0.219)	0.199 (0.345)	0.199 (0.345)	0.199 (0.355)
N2	−0.184 (−0.346)	−0.110 (−0.211)	−0.110 (−0.211)	−0.110 (−0.212)
N3	−0.184 (−0.339)	−0.142 (−0.303)	−0.141 (−0.289)	−0.142 (−0.275)
C4	0.040 (0.103)	0.054 (0.071)	0.054 (0.071)	0.054 (0.071)
C5	0.039 (0.105)	0.048 (0.073)	0.048 (0.074)	0.048 (0.074)
Atom	DCC	[CuCl(DCC)]	[CuBr(DCC)]	[CuI(DCC)]
C1	0.154 (0.210)	0.199 (0.327)	0.200 (0.326)	0.199 (0.325)
N2	−0.189 (−0.354)	−0.108 (−0.206)	−0.107 (−0.205)	−0.107 (−0.205)
N3	−0.182 (−0.329)	−0.142 (−0.325)	−0.142 (−0.311)	−0.144 (−0.287)
C4	0.032 (0.118)	0.046 (0.041)	0.046 (0.041)	0.046 (0.069)
C5	0.034 (0.074)	0.041 (0.110)	0.040 (0.112)	0.040 (0.098)

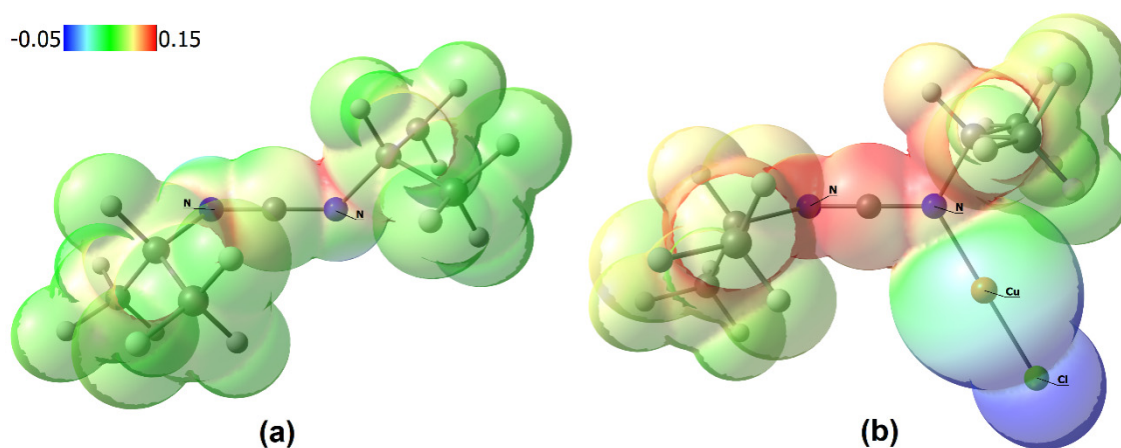


Figure 3. Overlapping sphere plots of (a) DICDI and (b) [CuCl(DICDI)] with mapped electrostatic potentials (a.u.).

4. Conclusions

DFT calculations confirmed that aliphatic carbodiimides such as DICDI and DCC can coordinate Cu(I) halides with the formation of linear complexes and that the interaction alters the orbital structure, the bond orders, and the electrophilicity, enhancing the reactivity towards nucleophiles. The CuX fragments essentially behave as Lewis acids, and the nature of X influences, to some extent, aspects such as the Cu–N bond strength, the carbodiimide→CuX donation, and the energies of frontier unoccupied orbitals. Despite the fact that CuCl is the most employed catalyst in combination with carbodiimides, some of the results provided in this study suggest that reactivity could be further enhanced by its replacement with CuI.

Funding: This research was funded by Università Ca' Foscari Venezia, grant D. R. 1065/2018 prot. 67416.

Institutional Review Board Statement: Not applicable.

Informed Consent Statement: Not applicable.

Acknowledgments: Università Ca' Foscari Venezia is gratefully acknowledged for financial support (Bando Spin 2018, D. R. 1065/2018 prot. 67416). We acknowledge CINECA (COLUMN project 2020) for the availability of high-performance computing resources.

References

1. Khorana, H.G. The Chemistry of Carbodiimides. *Chem. Rev.* **1953**, *53*, 145–166, doi:10.1021/cr60165a001.
2. Kurzer, F.; Douraghi-Zadeh, K. Advances in the Chemistry of Carbodiimides. *Chem. Rev.* **1967**, *67*, 107–152, doi:10.1021/cr60246a001.
3. Williams, A.; Ibrahim, I.T. Carbodiimide chemistry: Recent advances. *Chem. Rev.* **1981**, *81*, 589–636, doi:10.1021/cr00046a004.
4. Ulrich, A. *Chemistry and Technology of Carbodiimides*; Wiley: Chichester, UK, 2007.
5. Schmidt, E.; Moosmüller, F. Zur Kenntnis aliphatischer Carbodiimide. *Liebigs Ann. Chem.* **1956**, *597*, 235–240, doi:10.1002/jlac.19555970307.
6. Alexandre, C.; Rouessac, F. La dicyclohexylcarbodiimide, agent de deshydratation intramoléculaire des cetols. *Tetrahedron Lett.* **1970**, *11*, 1011–1012, doi:10.1016/S0040-4039(01)97893-1.
7. Schuster, E.; Hesse, C.; Schumann, D. Dehydration of 2-Hydroxyimines with Dicyclohexylcarbodiimide: An Access to Cyclic Alkenylimines. *Synlett* **1991**, 916–918, doi:10.1055/s-1991-20922.
8. Knochel, P.; Seebach, D. Dehydratisierung von Nitroaldolen mit Dicyclohexylcarbodiimid: Herstellung von Nitroolefinen unter milden Bedingungen. *Synthesis* **1982**, 1017–1018, doi:10.1055/s-1982-30045.
9. Mathias, L.J. Esterification and Alkylation Reactions Employing Isooureas. *Synthesis* **1979**, 561–576, doi:10.1055/s-1979-28761.
10. Gibson, F.S.; Sook Park, M.; Rapoport, H. Bis[[4-(2,2-dimethyl-1,3-dioxolyl)]methyl]-carbodiimide (BDDC) and Its Application to Residue-Free Esterifications, Peptide Couplings, and Dehydrations. *J. Org. Chem.* **1994**, *59*, 7503–7507, doi:10.1021/jo00103a054.
11. Sinha, S.; Ilankumaran, P.; Chandrasekaran, S. One pot conversion of alcohols to disulfides mediated by benzyltriethylammonium tetrathiomolybdate. *Tetrahedron* **1999**, *55*, 14769–14776, doi:10.1016/S0040-4020(99)00939-4.
12. Schur, C.; Becker, N.; Bergsträßer, U.; Hartung, J.; Gottwald, T. Tertiary alkoxy radicals from 3-alkoxythiazole-2(3H)-thiones. *Tetrahedron* **2011**, *67*, 2338–2347, doi:10.1016/j.tet.2010.12.071.
13. Kiełbasiński, P.; Żurawiński, R.; Orabowicz, J.; Mikołajczyk, M. Organosulphur compounds: XLVII Alkylation of sulphinic acids by o-alkylisoureas: O-versus s-reactivity and asymmetric synthesis of alkyl sulphinates. *Tetrahedron* **1988**, *44*, 6687–6692, doi:10.1016/S0040-4020(01)90108-5.
14. Bakibaev, A.A.; Shtrykova, V.V. Isooureas: Synthesis, properties, and applications. *Russ. Chem. Rev.* **1995**, *64*, 929–938, doi:10.1070/RC1995v064n10ABEH000185.
15. Bortoluzzi, M.; Paolucci, G.; Sartor, F.; Bertolasi, V. Synthesis and characterization of novel pyridine–isourea complexes of Pd(II). *Polyhedron* **2012**, *37*, 66–67, doi:10.1016/j.poly.2012.02.014.
16. Hartke, K.; Rossbach, F. Dimerisierung von Carbodiimiden. *Angew. Chem.* **1968**, *80*, 83, doi:10.1002/ange.19680800209.
17. Minenkov, Y.; Singstad, Å.; Occhipinti, G.; Jensen, V.R. The accuracy of DFT-optimized geometries of functional transition metal compounds: A validation study of catalysts for olefin metathesis and other reactions in the homogeneous phase. *Dalton Trans.* **2012**, *41*, 5526–5541, doi:10.1039/c2dt12232d.
18. Chai, J.-D.; Head-Gordon, M. Long-range corrected hybrid density functionals with damped atom–atom dispersion corrections. *Phys. Chem. Chem. Phys.* **2008**, *10*, 6615–6620, doi:10.1039/b810189b.
19. Gerber, I.C.; Ángyán, J.G. Hybrid functional with separated range. *Chem. Phys. Lett.* **2005**, *415*, 100–105, doi:10.1016/j.cplett.2005.08.060.

20. Weigend, F.; Ahlrichs, R. Balanced basis sets of split valence, triple zeta valence and quadruple zeta valence quality for H to Rn: Design and assessment of accuracy. *Phys. Chem. Chem. Phys.* **2005**, *7*, 3297–3305, doi:10.1039/b508541a.
21. Peterson, K.A.; Figgen, D.; Goll, E.; Stoll, H.; Dolg, M. Systematically convergent basis sets with relativistic pseudopotentials. II. Small-core pseudopotentials and correlation consistent basis sets for the post-d group 16–18 elements. *J. Chem. Phys.* **2003**, *119*, 11113–11123, doi:10.1063/1.1622924.
22. Li, Y.; Evans, J.N.S. The Fukui Function: A Key Concept Linking Frontier Molecular Orbital Theory and the Hard-Soft-Acid-Base Principle. *J. Am. Chem. Soc.* **1995**, *117*, 7756–7759, doi:10.1021/ja00134a021.
23. Cossi, M.; Rega, N.; Scalmani, G.; Barone, V. Energies, structures, and electronic properties of molecules in solution with the C-PCM solvation model. *J. Comput. Chem.* **2003**, *24*, 669–681, doi:10.1002/jcc.10189.
24. Barone, V.; Cossi, M. Quantum Calculation of Molecular Energies and Energy Gradients in Solution by a Conductor Solvent Model. *J. Phys. Chem. A* **1998**, *102*, 1995–2001, doi:10.1021/jp9716997.
25. Neese, F. The ORCA program system. *WIREs Comput. Mol. Sci.* **2012**, *2*, 73–78, doi:10.1002/wcms.81.
26. Neese, F. Software update: The ORCA program system, version 4.0. *WIREs Comput. Mol. Sci.* **2018**, *8*, e1327, doi:10.1002/wcms.1327.
27. Cramer, C.J. *Essentials of Computational Chemistry*, 2nd ed.; Wiley: Chichester, UK, 2004.
28. Hirshfeld, R.F. Bonded-atom fragments for describing molecular charge densities. *Theor. Chim. Acta* **1977**, *44*, 129–138, doi:10.1007/BF00549096.
29. Mayer, I. Charge, bond order and valence in the AB initio SCF theory. *Chem. Phys. Lett.* **1983**, *97*, 270–274, doi:10.1016/0009-2614(83)80005-0.
30. Sizova, O.V.; Skripnikov, L.V.; Sokolov, A.Y. Symmetry decomposition of quantum chemical bond orders. *J. Mol. Struct.* **2008**, *870*, 1–9, doi:10.1016/j.theochem.2008.08.021.
31. Bader, R.F.W. A quantum theory of molecular structure and its applications. *Chem. Rev.* **1991**, *91*, 893–928, doi:10.1021/cr00005a013.
32. Dapprich, S.; Frenking, G. Investigation of Donor-Acceptor Interactions: A Charge Decomposition Analysis Using Fragment Molecular Orbitals. *J. Phys. Chem.* **1995**, *99*, 9352–9362, doi:10.1021/j100023a009.
33. Gorelsky, S.I.; Ghosh, S.; Solomon, E.I. Mechanism of N₂O Reduction by the μ_4 -S Tetranuclear Cu₂ Cluster of Nitrous Oxide Reductase. *J. Am. Chem. Soc.* **2006**, *128*, 278–290, doi:10.1021/ja055856o.
34. Lu, T.; Chen, F. Multiwfn: A multifunctional wavefunction analyzer. *J. Comput. Chem.* **2012**, *33*, 580–592, doi:10.1002/jcc.22885.